Dalton Transactions

ROYAL SOCIETY OF CHEMISTRY

PAPER

View Article Online
View Journal

Cite this: DOI: 10.1039/d5dt02844b

Crystallographic evidence of a trinuclear (salen)manganese(IV/III/IV)–μ-oxo formed during catalytic C(sp^3)–H oxidation reactions

Bhaswati Paul, [a] Kusalvin Dabare, [a,b] Joshua D. Bocarsly[a,b] and L. Reginald Mills *[a]

Received 27th November 2025,
Accepted 10th December 2025

DOI: 10.1039/d5dt02844b

rsc.li/dalton

The formation of manganese–oxo catalysts involved in C(sp^3)–H bond oxidation was explored in the targeted synthesis of (salen/salophen)manganese complexes that varied axial ligand identity and varied oxidation state of the manganese center. Isolated compounds included dinuclear (salen/salophen)manganese(III)–μ-hydroxo and trinuclear (salen)manganese(IV/III/IV)–μ-oxo, the latter of which formed by oxidation with catalytically relevant oxidant iodosylbenzene. The X-ray structure of trinuclear complex (salen)manganese(IV/III/IV)–μ-oxo indicated a Mn(IV)–O–Mn(III)–O–Mn(IV) motif, with nearly linear Mn–O–Mn angles of 166.19(12)° and 172.47(15)°, Mn(IV)–O bond lengths of 1.948(2) and 1.998(2) Å, and Mn(III)–O bond lengths of 2.102(2) and 2.118(2) Å. All well-defined (salen/salophen)manganese hydroxo and oxo compounds served as precatalysts for oxidation of C(sp^3)–H substrates 9,10-dihydroanthracene (>99% conversion), fluorene (52–70% conversion), and phenylcyclohexane (with lower 18–23% conversion), albeit with lower rate of activity for the isolated trinuclear μ-oxo compound, allowing its assignment as an off-cycle catalyst aggregate. These data supported the proposal of a manganese(III/V) cycle for C(sp^3)–H oxidation, which involved monomerization of the dinuclear (salen)manganese(III)-μ-hydroxo catalyst prior to rate-determining C(sp^3)–H activation.

Introduction

C–H functionalization reactions entail direct transformations of unfunctionalized molecules,[1] providing a way to rapidly diversify organic compounds.[2] Among strategies for C–H functionalization, reactions that employ hydrogen atom transfer (HAT) enable the activation of C(sp^3)-hybridized positions, without the need for directing groups.[3] While C(sp^3)–H functionalization reactions by free radical intermediates have been long-established in synthetic organic chemistry, many free radicals are inherently reactive and poorly selective for molecules with many C–H bonds.[4] Instead of free radical-initiated HAT reactions, an alternative strategy entails the use of transition metal metalloradical catalysts,[5] which mimic the reactivity of free-radical intermediates,[6] however enable selective catalytic C–H functionalization *via* steric and electronic modulation of the supporting ligand.

Among metalloradical catalysts for C(sp^3)–H functionalization, early chemistry from Kochi and workers demonstrated that salicylaldehyde–ethylamine (salen)-supported manganese complexes catalyzed the C–H oxidation of cyclohexane in the presence of iodosylbenzene.[7] A range of catalytic manganese systems have also been demonstrated for metalloradical C(sp^3)–H functionalization,[8] most prominently (porphyrin)manganese catalysts,[9] for instance in undirected C(sp^3)–H halogenation[10,11] and azidation reactions,[12] additionally with lower catalyst loadings compared to prototypical (salen)manganese catalysts.[13]

A generally proposed mechanism for (salen)manganese(III)-catalyzed C–H oxidation involves generation of (salen)manganese(V)–oxo, which is the reactive catalytic intermediate for C–H oxidation *via* hydrogen atom abstraction (Scheme 1).[14,15] The study of oxomanganese intermediates involved in C–H oxidation has been of interest,[16] although the inherently reactive nature of these catalytic intermediates can render isolation challenging.[17,18] Early *in situ* characterization of relevant oxomanganese and hydroxomanganese intermediates has been aided by rapid analytical techniques, for instance spectroscopic detection of (porphyrin)oxomanganese(V) intermediates;[19] as well as mass spectrometric detection of (salen)oxomanganese(V) intermediates.[20,21] For the isolation of oxomanganese intermediates, synthetic strategies have generally involved sterically demanding supporting ligands that protect the metal center, for instance on the (porphyrin)oxomanganese(V) class,[22] or in the non-heme oxomanganese(IV/V) class.[23]

[a]Department of Chemistry, University of Houston, Houston, TX 77204-5003, USA
[b]Texas Center for Superconductivity, University of Houston, Houston, TX 77204, USA. E-mail: lrmills2@uh.edu

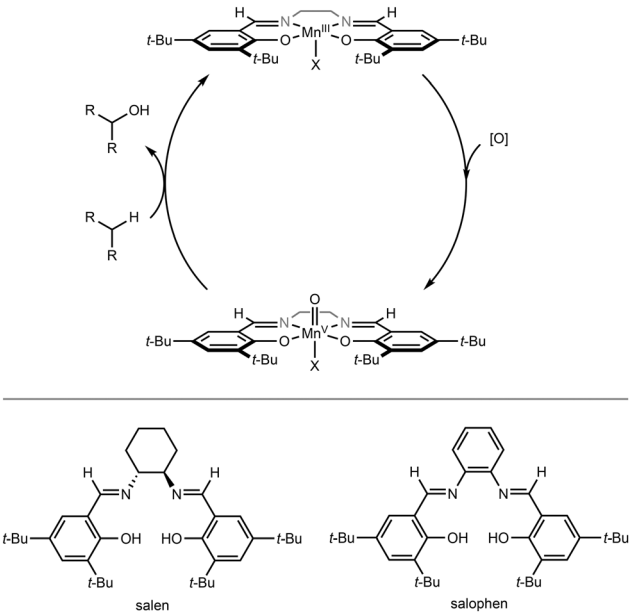

Scheme 1 Generally proposed mechanism for (salen/salophen)manganese-catalyzed C(sp^3)–H oxidation.

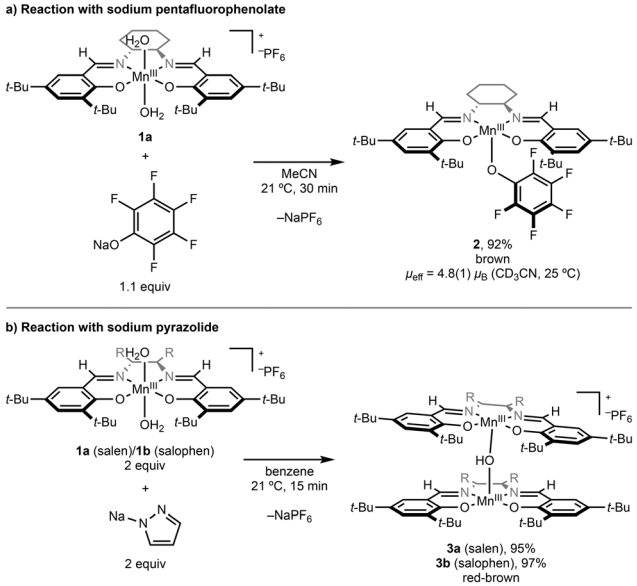

Scheme 2 Reactions of (salen/salophen)Mn(III) compounds with (a) sodium pentafluorophenolate and with (b) sodium pyrazolate.

Among (salen)oxomanganese complexes, isolated oxos are fewer, with notable examples including the sterically demanding, mononuclear (salen)manganese(IV)–hydroxo of Fujii and coworkers,[24,25] and the dimeric (salen)manganese(IV)–di-μ-oxo of Fujii and coworkers.[26–28]

For (salen)manganese C–H oxidation catalysts, outstanding questions include the significance of axial ligand identity (ligand = X in Scheme 1),[29,30] especially of type hydroxo, with other systems demonstrating competence of hydroxomanganese complexes for C–H abstraction.[31] Namely, while axial ligand identity is proposed to be relevant in the single-step hydrogen atom abstraction reaction of oxomanganese intermediates,[32] the impact of axial ligand towards (salen)manganese catalyst turnover is more ambiguous, especially if axial ligand is exchangeable in a complex catalytic mixture. To better understand reactive (salen)manganese intermediates involved in C(sp^3)–H oxidation,[7,13] herein is reported the targeted synthesis of (salen)manganese-hydroxo and -oxo complexes derived of Jacobsen's catalyst, the reactivity of the isolated compounds towards organic C(sp^3)–H substrates in the presence of iodosylbenzene, and insights into the speciation of (salen)oxomanganese during catalysis.

Results and discussion

In the interest of exploring the reactivity of salen-supported manganese catalysts for C(sp^3)–H oxidation, initial syntheses explored variation of the axial ligand of the catalyst complex (Scheme 2), which was proposed to affect the reactivity of oxomanganese catalytic intermediates.[33] Beginning with cation (salen)manganese(III) bis-aqua derived of Jacobsen's catalyst (**1a**), ligand exchange with sodium pentafluorophenolate resulted in formation of brown solid with identity (salen)manganese(III) pentafluorophenoxide (**2**) (Scheme 2a). The structure of (salen)manganese(III) pentafluorophenoxide (**2**) determined by single crystal X-ray diffraction evidenced a mononuclear complex (**2**) obtained in 92% isolated yield, with a Mn1–OC_6F_5 bond length of 2.0664(15) Å. Dissolution of the material in benzene-d_6 and analysis by ^{1}H NMR spectroscopy demonstrated broad paramagnetic resonances between 17.52 and −26.45 ppm,[34] and the complex exhibited a solution-state magnetic moment of 4.8(1)μ_B, altogether consistent with a high-spin (S = 2) (salen)manganese(III) complex.[35]

Analogous ligand exchange was targeted using sodium pyrazolate in reactions with (salen)manganese(III) cation (**1a**) and with (salophen)manganese(III) cation (**1b**), which resulting in formation of red-brown products (Scheme 2b). Determination of the molecular structures of **3a**/**3b** by X-ray diffraction indicated formation of dimanganese(III) μ-hydroxo monocation complexes (salen/salophen)Mn–(μ-OH)–(salen/salophen)Mn(PF_6) (Scheme 2b), reminiscent of the μ-hydroxo triflate complex (salen)Mn(III)–(μ-OH)–(salen)Mn(III)(OTf) synthesized by Kurahashi.[36,37] In the solid-state structure of the salophen derivative (**3b**), cocrystallization of two dimanganese(III) μ-hydroxo monocations was observed (Fig. S21), one of which bore a capping pyrazole ligand (**3b**-PzH) (Fig. 1). The X-ray structure of **3b**-PzH indicated two manganese(III) centers, a bridging OH group, and a single pyrazole ligand. For the **3b**-PzH molecule, the measured Mn–OH bond lengths were 1.991(2) Å and 2.094(2) Å, with a Mn1–O(H)–Mn2 angle of 153.32(14)°, similar to the μ-hydroxo octaethylporphyrinato complex of Fries, Marchon, Scheidt, and coworkers, (OEP)Mn(III)–(μ-OH)–(OEP)Mn(III), which displayed a Mn–O(H)–Mn bridge angle of 152.73(11)°.[38,39] For the current complex

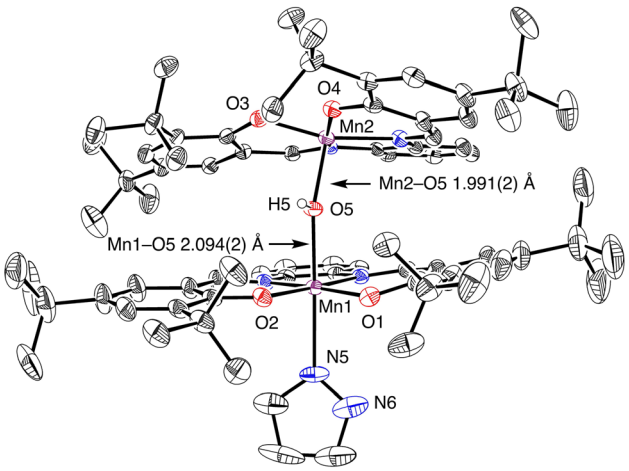

Fig. 1 Solid-state molecular structure of pyrazole-coordinated (salophen)Mn–(μ-OH)–(salophen)Mn(PzH)(PF_6) cation (**3b**-PzH) determined by X-ray diffraction (30% probability ellipsoids). H atoms, solvent molecules, PF_6 counterion, and cocrystallizing molecule of **3b** omitted for clarity (see SI for details). Hydrogen atom H5 was located and freely refined. Select bond lengths (Å) and angles (°): Mn1–O5 2.094(2); Mn2–O5 1.991(2); Mn1–N5 2.318(4); Mn1–O5–Mn2 153.32(14).

(**3b**-PzH), the longer Mn1–N5 bond length of 2.318(4) Å was consistent with weaker manganese(III)–pyrazole coordination, with the pyrazole proposed to undergo dynamic ligand exchange in solution. Dissolution of **3a**/**3b** in benzene-d_6 and analysis by ^{1}H NMR spectroscopy indicated broadened signals between 16.46 and −21.71 ppm, consistent with paramagnetic character for the manganese(III)–μ-OH-manganese(III) complexes (**3a**/**3b**). In benzene-d_6 solution at 298 K, the observed magnetic moments were 5.4(1)μ_B for **3a** and 5.2(1)μ_B for **3b**, lower than the expected spin-only value of 6.9μ_B for two noninteracting S = 2 Mn(III) centers. In the solid-state, variable temperature SQUID magnetometry for **3b** modelled the antiferromagnetic coupling at isotropic g = 2.00 with J = −28.80(3) cm^{-1}, consistent with the coupling observed in related manganese(III)–μ-hydroxo compounds (Fig. 2).[40–42] Together, these data evidenced that reaction of (salen/salophen)manganese(III) bis-aqua cation (**1a**/**b**) with sodium pyrazolate resulted in water ligand deprotonation rather than pyrazolate coordination,

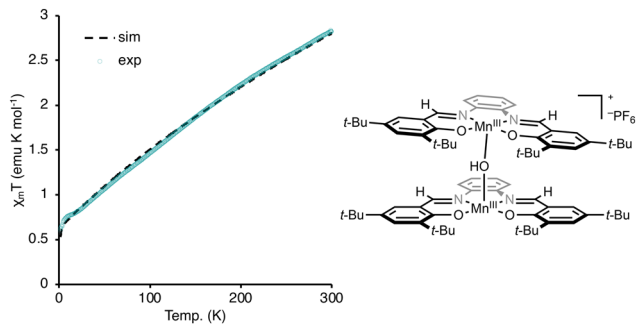

Fig. 2 Variable-temperature SQUID magnetization for (salophen)Mn–μ-OH–(salophen)Mn(PF_6) (**3b**) recorded in the solid state. Magnetic field = 200 Oe. Simulation parameters: g_{iso} = 2.00, J = −28.80(3) cm^{-1}.

forming the hydroxo-bridged dimanganese(III) complex. Compared to ligand association reaction of less basic sodium pentafluorophenolate (**2**) (pK_a of C_6F_5OH = 5.5 in H_2O),[43] these data demonstrate that (salen/salophen)manganese(III) bis-aqua cation is more acidic than pyrazole (pK_a = 19.8 in DMSO),[44] undergoing deprotonation by basic ligands and limiting the options for synthesis of complexes by ligand exchange with such basic ligands.

The deprotonation of (salen)manganese(III) bis-aqua cation (**1a**) with sodium pyrazolate can be compared with the same deprotonation employing aqueous KOH instead of NaPz, reported by Fujii and coworkers to form dimanganese(IV) di-μ-oxo (**4**) in the presence of air.[26] Repeating the procedure of Fujii and coworkers employing 1,8-diazabicyclo[5.4.0]undec-7-ene (DBU) as base in acetonitrile open to air, full conversion of bis-aqua complex (**1a**) was determined by ^{1}H NMR spectroscopy in acetonitrile-d_3 (eqn (1)), with the identity of the product verified by X-ray diffraction (Fig. S26).[26,45] These results demonstrate that deprotonation of bis-aqua complex (**1a**) in the presence of air results in oxidation to a di-μ-oxo, which is distinct from the desired terminal (salen)manganese (V)–oxo catalytic intermediate often proposed in C(sp^3)–H oxidation reactions.

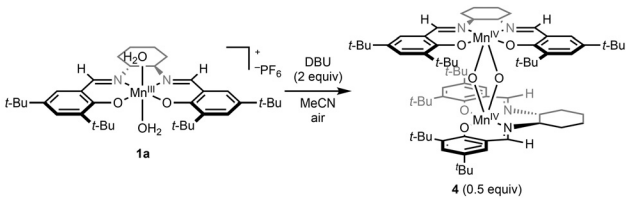

(1)

After isolation of (salen/salophen)manganese(III)–μ-hydroxo compounds (**3a**/**3b**), the synthesis of higher oxidation state (salen)manganese complexes relevant to C–H oxidation was targeted (Scheme 3). In a one-pot procedure, after formation of (salen)manganese(III)–μ-hydroxo (**3a**), treatment with oxidant iodosylbenzene under air resulted in conversion to a crystalline brown solid (**5**), which displayed broad paramagnetic resonances between 11.64 and −14.29 ppm by ^{1}H NMR spectroscopy in acetonitrile-d_3 (Scheme 3). After isolation of single crystals suitable for X-ray diffraction, the solid-state structure was determined to be a trinuclear monocationic complex consisting of two oxidized (salen)manganese(IV) centers at the ends (Mn1, Mn3), a (salen)manganese(III) atom in the middle (Mn2), and two μ-oxos (O1, O2) bridging the (salen)manganese atoms (Fig. 3).[46] The manganese(IV)–oxo bond lengths (1.998(2) Å, 1.948(2) Å) were shorter than the manganese(III)–oxo bond lengths (2.102(2) Å, 2.118(2) Å), consistent with Mn(IV)=O double-bond character and Mn(III)–O single-bond character, which was apparent in the direct comparison of Mn–O(H/R) bond lengths for the series of complexes (salen)Mn(III)$(OH_2)_2$, **2**, **3a**, and **5** (Table 1). Comparison of these complexes also informed highly conserved bond lengths across the organic salen ligand framework (O–C_{aryl} and $O_{aryl}C$=CC_{imine}), demonstrating identical electronic structures on the salen sup-

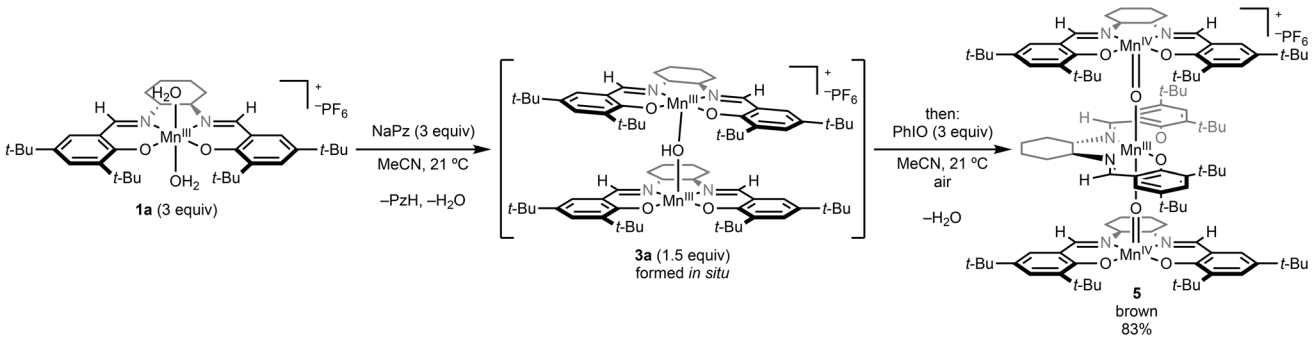

Scheme 3 Synthesis of trinuclear (salen)manganese(IV/III/IV)–μ-oxo (**5**).

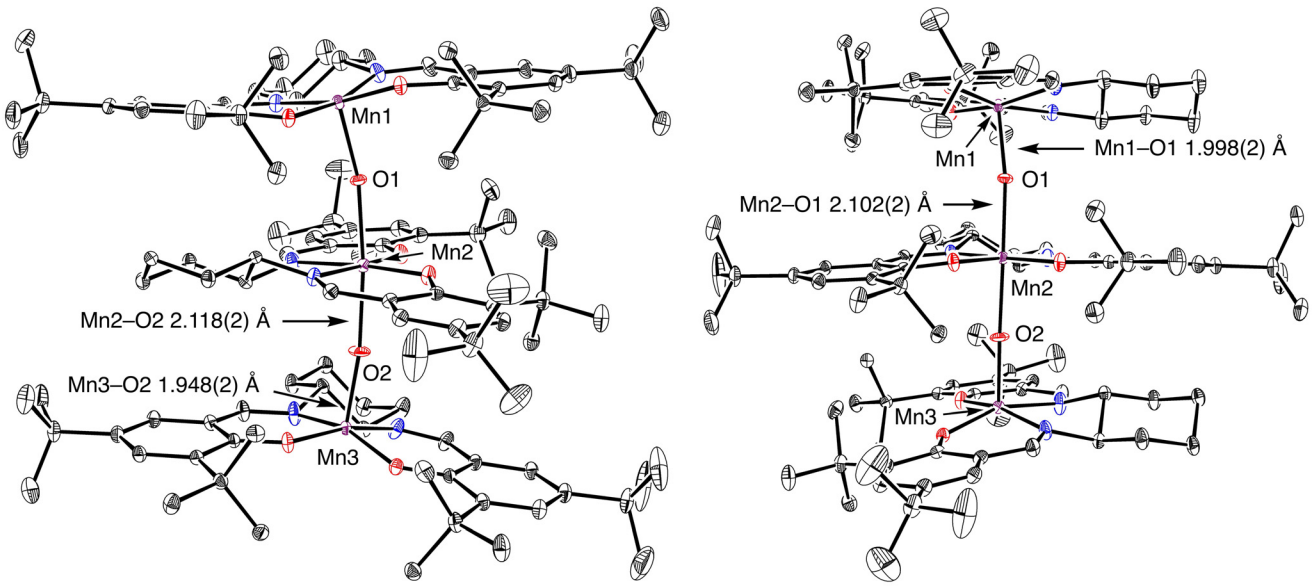

Fig. 3 Front-view (left) and side-view (right) of the solid-state molecular structure of **5** determined by single crystal X-ray diffraction (30% probability ellipsoids). H atoms, solvent molecules, and PF_6 counterion omitted for clarity. Select bond-lengths (Å) and angles (°): Mn1–O1 1.998(2); Mn2–O1 2.102(2); Mn2–O2 2.118(2); Mn3–O2 1.948(2); Mn1–O1–Mn2 166.19(12); Mn2–O2–Mn3 172.47(15).

Table 1 Selected bond lengths (Å) for (salen)manganese complexes determined by X-ray diffraction

Compound	Mn–O(H/R)	O_{Aryl}–Mn	N_{Imine}–Mn	O–C_{Aryl}	$O_{Aryl}C{=}CC_{Imine}$
(salen)Mn(OH_2)(dioxane)(ClO_4)[48]	2.269	1.860	1.979	1.329	1.409
		1.860	1.980	1.316	1.400
2	2.0664(15)	1.8692(15)	1.9773(16)	1.321(2)	1.418(3)
		1.8747(14)	1.9909(18)	1.329(3)	1.418(3)
3a	2.0355(18)	1.868(3)	1.998(4)	1.336(6)	1.413(7)
		1.869(4)	1.973(4)	1.331(6)	1.409(7)
5	1.998(2)	1.870(2)	1.979(3)	1.318(4)	1.417(4)
	2.102(2)	1.879(2)	1.986(3)	1.319(4)	1.414(4)
	2.118(2)	1.892(2)	1.994(3)	1.314(4)	1.417(4)
	1.948(2)	1.877(2)	1.986(3)	1.315(4)	1.418(4)
		1.882(2)	1.979(3)	1.320(4)	1.423(5)
		1.866(2)	1.972(3)	1.317(4)	1.422(4)

porting ligand, with any electronic differences between complexes occurring primarily at the manganese center (Table 1). The Mn(IV/III/IV) assignment of (salen)manganese(IV/III/IV)–μ-oxo compound (**5**) was further corroborated by a Mn 3s doublet separation of 5.0 eV measured by XPS (Fig. S61),[47] demonstrating (salen)manganese(IV/III/IV)–μ-oxo (**5**) to be the thermodynamic product of (salen)manganese(III)–μ-hydroxo (**3a**) oxidation using iodosylbenzene.

The formation of (salen)manganese(IV/III/IV)–μ-oxo (**5**) was rationalized by an oxidation/comproportionation sequence (Scheme 4). Namely, upon treatment of (salen)manganese (III)–μ-hydroxo (**3a**) with PhIO, the initial product of (salen) manganese oxidation is proposed to be terminal (salen) manganese(V)–oxo (**6a**). In the presence of excess (salen) manganese(III) (**3a**), comproportionation, proton transfer, and ligand redistribution generates trinuclear (salen)manganese(IV/III/IV)–μ-oxo (**5**), which precipitates from solution as a crystalline brown solid, concomitant with (salen)manganese(III) cation (**1a**) that can further react with excess sodium pyrazolate and iodosylbenzene. These reactions establish kinetically accessible axial ligand exchange after reaction with iodosylbenzene, indicating formation of thermodynamic oxidized (salen) manganese products according to presence of oxidant.

In the solid state, variable temperature SQUID magnetization measured for (salen)manganese(IV/III/IV)–μ-oxo (**5**) established significant antiferromagnetic coupling between the three high-spin manganese centers, simulated at isotropic g = 2.00 with a coupling constant of J = −61.1(2) cm^{-1} (Fig. 4). This value was comparable to the coupling observed for other manganese(IV/III)–μ-oxos,[49,50] and compared to the (salophen) manganese(III)–μ-hydroxo (**3b**, J = −28.80(3) cm^{-1}) is consistent with more significant superexchange interaction expected for the bridging μ-oxo (**5**).[42] The solid state moment matched the acetonitrile-d_3 solution-state magnetic moment of μ_{eff} = 5.4 (1)μ_B at 298 K, consistent with antiferromagnetic coupling and fidelity of the trinuclear complex upon dissolution in acetonitrile-d_3. This fidelity was exemplified upon incubation of equimolar (salen)manganese(IV/III/IV)–μ-oxo (**5**) with (salophen) manganese–μ-hydroxo (**3b**) in acetonitrile-d_3 at ambient temperature, which resulted in no apparent ligand exchange between the complexes by ^{1}H NMR spectroscopy after 1 h (Fig. S35). These data altogether indicate that trinuclear

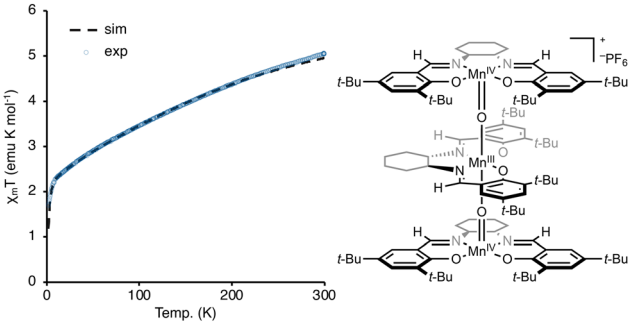

Fig. 4 Temperature-dependent SQUID magnetization for (salen)Mn(IV/III/IV)–μ-oxo (**5**) recorded in the solid state. Magnetic field = 200 Oe. Simulation parameters: g_{iso} = 2.00, J = −61.1(2) cm^{-1}.

(salen)manganese(IV/III/IV)–μ-oxo (**5**) is a thermodynamic, stable product of (salen)manganese(III)–μ-hydroxo oxidation.

With some isolated (salen)manganese compounds in hand, their relevance was determined in C(sp^3)–H oxidation reactions employing iodosylbenzene, demonstrating that all isolated compounds served as precatalysts (Table 2). As model reaction in 9 : 1 acetonitrile/water mixture open to air, one equivalent of the suitable C–H substrate, three equivalents of oxidant, and 10 mol% (per Mn center) of the appropriate (salen/salophen) manganese compound were stirred at ambient temperature until reaction progression halted, as judged by GC-MS analysis of reaction aliquots. Both PF_6 bis-aqua cations (salen)manganese (**1a**) and (salophen)manganese (**1b**) gave similar reactivity, with full conversion of 9,10-dihydroanthracene (DHA), 68–70% conversion of fluorene, and partial conversion (20–22%) of phenylcyclohexane (Table 2, entries 1 and 2). Employing 10 mol% per Mn center of newly isolated (salen/salophen) manganese compounds (**2**, **3a–b**, **5**) resulted in comparable conversions of the three substrates in all cases (±15%) (entries

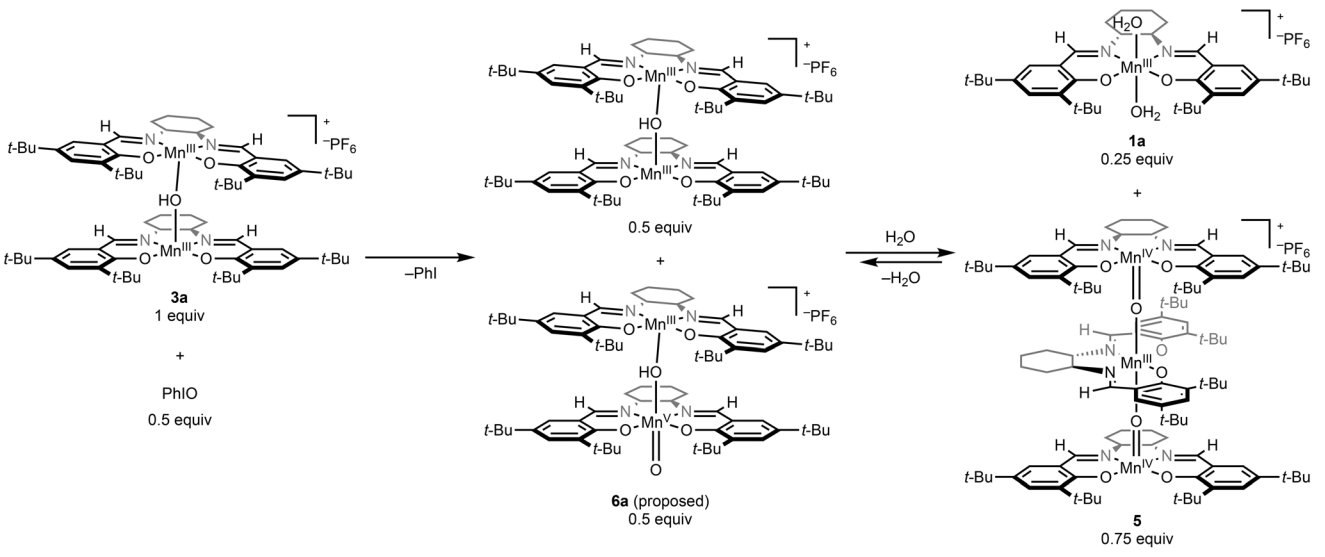

Scheme 4 Rationalized intermediates leading to trinuclear complex formation.

Table 2 Evaluation of well defined salen/salophen Mn catalysts for C–H oxidation

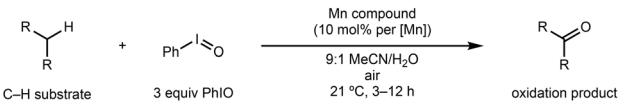

		C–H substrate conversion[a]		
Entry	Mn compound	DHA	Fluorene	CyPh
1	**1a** (10 mol%)	>99%[b]	68%	20%
2	**1b** (10 mol%)	>99%	70%	22%
3	**2** (10 mol%)	>99%	80%	18%
4	**3a** (5 mol%)	>99%[c]	52%	22%
5	**3b** (5 mol%)	>99%	58%	23%
6	**5** (3.3 mol%)	>99%[d]	65%	18%

[a] Conversions determined by GC-MS. DHA = 9,10-dihydroanthracene. [b] KIE($^{1/2}$H) = 3.1(6). [c] KIE($^{1/2}$H) = 1.9(2). [d] KIE($^{1/2}$H/D) = 3.1(3).

3–6). Importantly, these data demonstrated the catalytic competence of (salen/salophen)manganese μ-hydroxo (**3a–b**) and (salen)manganese(IV/III/IV) μ-oxo (**5**) compounds, the latter of which was synthesized with the catalytically relevant oxidant, iodosylbenzene. Together, these results implicated the observed coordination chemistry of μ-hydroxo (**3a–b**) and μ-oxo (**5**) as reflecting the coordination chemistry of the active (salen)manganese catalyst that engages turnover-limiting C(sp^3)–H oxidation.

The catalytic competence of (salen)manganese complexes of different nuclearity (**1a**, **3a**, **5**) raised a question about catalyst nuclearity, since studies thus far indicated that isolated dinuclear (**3a**/**b**) and trinuclear (**5**) compounds were metastable in acetonitrile-d_3 solution as determined by ^{1}H NMR spectroscopy. Namely, when starting from different precatalysts (**1a**, **3a**, **5**), could the same C(sp^3)–H oxidation catalysts be generated *in situ*, or would different catalysts be formed in all cases? By UV-vis absorption spectroscopy, discrimination of the isolated (salen)manganaese compounds was apparent, with (salen)manganese(III) cation (**1a**) exhibiting a peak at 367 nm, and both (salen)manganese(III)–μ-hydroxo (**3a**) and (salen)manganese(IV/III/IV)–μ-oxo (**5**) exhibiting peaks at 420 nm (Fig. 5a). When using the isolated compounds (**1a**, **3a**, **5**) as precatalysts for oxidation of DHA with PhIO, the UV-vis spectra of the catalytic reaction mixtures were identical, exhibiting a conserved peak at 445 nm, indicating identical catalyst speciation regardless of initial axial ligand identity (Fig. 5b). In parallel time courses, the initial rates of 9,10-DHA conversion were also comparable between precatalysts, with parent (salen) manganese(III) cation (**1a**) displaying a slightly faster rate (*ca.* 2.9 times faster than **5**) (Fig. 5c). While the precise identity of the active catalyst for C(sp^3)–H oxidation was not apparent from spectroscopic studies, initial rate kinetics indicated approximate first-order dependence according to initial concentration of **1a**, and partial order dependence on concentration of [Mn] center when employing either **3a** or **5**, implying that dinuclear and trinuclear intermediates are not directly active for rate-determining C(sp^3)–H activation, with monomerization preceding the C(sp^3)–H activation step (Fig. S57–S59). Altogether, these data further support the observed coordination chemistry of (salen)manganese complexes, which undergo oxidation with iodosylbenzene and subsequently undergo rapid intermolecular axial ligand exchange, leading to the catalytic resting state. For (salen)manganese(IV/III/IV)–μ-oxo (**5**) in particular, while it is a thermodynamic product of (salen)manganese oxidation by iodosylbenzene, it alone was not kinetically competent for oxidation of 9,10-DHA in a stoichiometric reaction (Fig. S36). Therefore, **5** is more accurately described as an off-cycle catalyst aggregate, which forms in the comproportionation of (salen)manganese(V)-oxo with excess (salen)manganese(III) cation when C(sp^3)–H substrate and/or oxidant are depleted.

Finally, the catalytic competence of (salen)manganese(III)-μ-hydroxo cation (**3a**) allowed proposal of a simplified catalytic

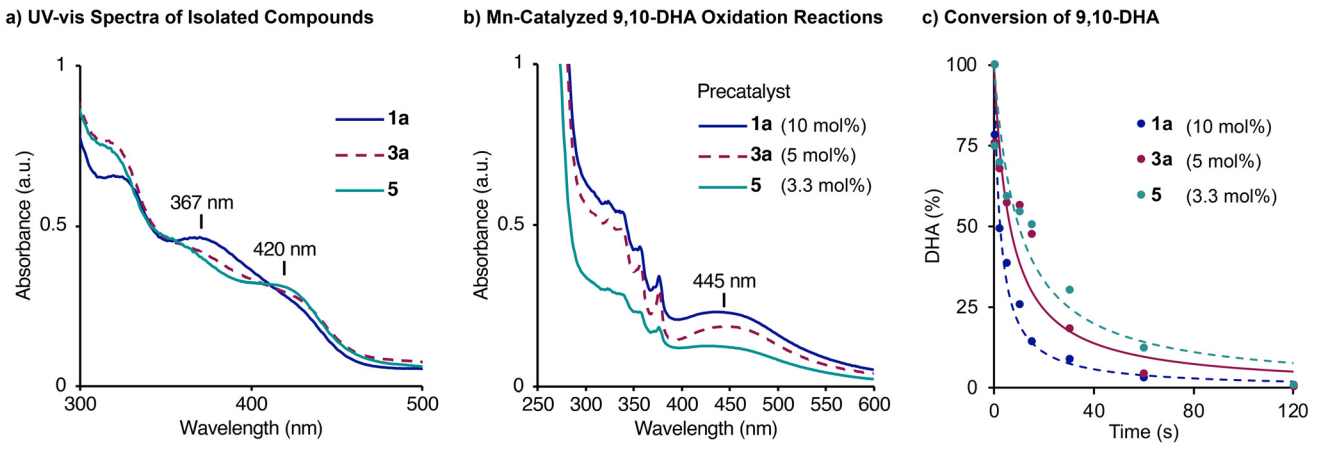

Fig. 5 (a) UV-vis absorption spectra of **1a** (100 μM) (red), **3a** (50 μM) (blue), and **5** (33 μM) (green) in acetonitrile. (b) UV-Vis spectra of (salen)manganese-catalyzed DHA oxidation (*ca.* 15% conversion) initiated from 10 mol% **1a**, 5 mol% **3a**, and 3.3 mol% **5** in acetonitrile/water (9 : 1). (c) Concentration of 9,10-DHA over time according to precatalyst in reaction with PhIO (3 equiv.); lines represent least-squares fit to a standard kinetic model.

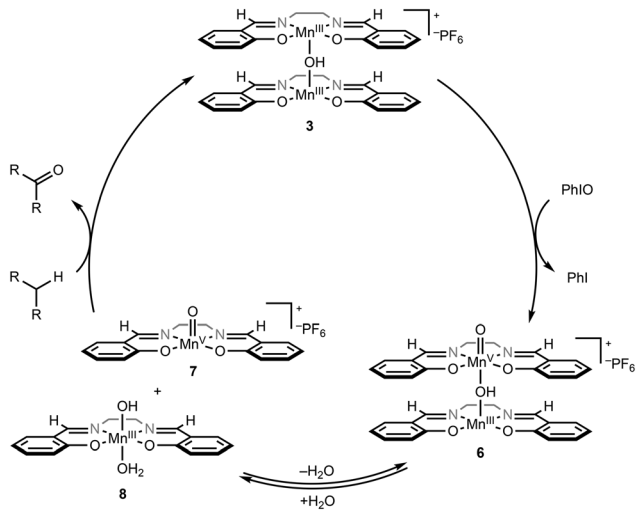

Scheme 5 Simplified catalytic cycle for (salen)Mn(μ-OH)-catalyzed C–H oxidation.

cycle for C(sp^3)–H oxidation (Scheme 5).[51] Namely, the synthesis of (salen)manganese(III)-μ-hydroxo cation (**3a**) evidenced dimerization of the complex prior to oxidation by PhIO. Thus, the starting dimeric μ-hydroxo (**3**) is oxidized, which initially yields dinuclear (salen)oxomanganese (**6**) (Scheme 5). Dinuclear (salen)oxomanganese intermediates (**6**) have previously been proposed as reservoir species for catalytically active mononuclear (salen)manganese(V)–oxo (**7**),[21] which dissociation is proposed to occur in the presence of coordinating solvent.[17] Then, turnover-limiting C–H oxidation regenerates (salen)manganese(III) (**3**), completing the cycle.

Conclusions

To investigate (salen)manganese intermediates in C(sp^3)–H oxidation, the reaction of (salen)manganese(III)–μ-hydroxo with iodosylbenzene formed trinuclear (salen)manganese(IV/III/IV)–μ-oxo, which was rationalized as a comproportionation product of a (salen)manganese(V)–oxo intermediate with well defined (salen)manganese(III) cation. The isolated (salen)manganese(IV/III/IV)–μ-oxo compound initiated C(sp^3)–H oxidation reactions, evidencing manganese–oxo formation as being catalytically relevant. While manganese–oxo formation has been previously proposed or observed with other manganese catalysts, the current compound represents a rare manganese(IV)–μ-oxo on the salen platform that was isolated and characterized crystallographically.

The observed complexes also evidenced thermodynamically favorable dimerization of manganese(III)–μ-hydroxo and manganese(IV/III/IV)–μ-oxo complexes *via* Mn–O–Mn bridging interactions in the solid state. While oxomanganese intermediates are often drawn as monomeric in C(sp^3)–H oxidation reactions, notably many structurally characterized monomeric oxomanganese compounds bear sterically demanding supporting ligands, which may inhibit intermolecular association. Herein, structural characterization was performed on the catalytically relevant (salen)manganese platform derived of commonly employed Jacobsen's catalyst, and the observation of dinuclear and trinuclear complexes with this ligand evidenced that catalysts for C(sp^3)–H oxidation may favor aggregation, especially in the absence of productive reactions when substrate or reagent is depleted. Finally, whereas axial ligand identity is proposed to affect the rate of a C–H abstraction step by oxomanganese complexes, herein the axial ligand identity of the (salen)manganese precatalyst bore no apparent impact on catalyst resting state or turnover number, evidencing rapid axial ligand exchange and kinetically accessible (salen)manganese catalyst speciation regardless of precatalyst axial ligand.

Author contributions

B. P. and L. R. M. conceived the work and designed experiments. B. P. performed all experiments. K. D. and J. D. B. assisted with initial collection of SQUID magnetization data. The manuscript was written by all authors.

Conflicts of interest

The authors declare no competing financial interest.

Data availability

Full experimental details and characterization are available in the supplementary information (SI). Supplementary information: general experimental considerations, experimental procedures, spectral characterization data, and supplemental X-ray crystallographic data. See DOI: https://doi.org/10.1039/d5dt02844b.

CCDC 2483878–2483882 contain the supplementary crystallographic data for this paper.[52a–e]

Acknowledgements

The Texas University Fund is acknowledged for University of Houston start-up funding. J. D. B. acknowledges support from the Welch Foundation (E-2179-20240404). Dr Boris Makarenko (University of Houston) is thanked for assistance with XPS analysis.

References

1 (*a*) N. Y. S. Lam, K. Wu and J.-Q. Yu, *Angew. Chem., Int. Ed.*, 2021, **60**, 15767–15790; (*b*) T. Dalton, T. Faber and F. Glorius, *ACS Cent. Sci.*, 2021, **7**, 245–261.
2 L. Guillemard, N. Kaplaneris, L. Ackermann and M. J. Johansson, *Nat. Rev. Chem.*, 2021, **5**, 522–545.

3 M. C. White and J. Zhao, *J. Am. Chem. Soc.*, 2018, **140**, 13988–14009.
4 D. L. Golden, S.-E. Suh and S. S. Stahl, *Nat. Rev. Chem.*, 2022, **6**, 405–427.
5 M. R. Bermejo, A. Castiñeiras, J. C. Garcia-Monteagudo, M. Rey, A. Sousa, M. Watkinson, C. A. McAuliffe, R. G. Pritchard and R. L. Beddoes, *J. Chem. Soc., Dalton Trans.*, 1996, **1996**, 2935–2944.
6 J. M. Mayer, *Acc. Chem. Res.*, 2011, **44**, 36–46.
7 (*a*) K. Srinivasan, P. Michaud and J. K. Kochi, *J. Am. Chem. Soc.*, 1986, **108**, 2309–2320; (*b*) K. Srinivasan, S. Perrier and J. K. Kochi, *J. Mol. Catal.*, 1986, **36**, 297–317.
8 (*a*) M. Guo, T. Corona, K. Ray and W. Nam, *ACS Cent. Sci.*, 2019, **5**, 13–28; (*b*) G. Olivo, O. Lanzalunga and S. Di Stefano, Imine-based Iron and Manganese Complexes as Catalysts for Alkane Functionalization, in *Alkane Functionalization*, ed. A. J. L. Pombeiro and M. F. C. G. da Silva, Wiley, 2018, pp. 231–249.
9 (*a*) B. Meunier, *Chem. Rev.*, 1992, **92**, 1411–1456; (*b*) R. A. Baglia, J. P. T. Zaragoza and D. P. Goldberg, *Chem. Rev.*, 2017, **117**, 13320–13352.
10 W. Liu and J. T. Groves, *J. Am. Chem. Soc.*, 2010, **132**, 12847–12849.
11 W. Liu, X. Huang, M.-J. Cheng, R. J. Nielsen, W. A. Goddard and J. T. Groves, *Science*, 2012, **337**, 1322–1325.
12 W. Liu and J. T. Groves, *Acc. Chem. Res.*, 2015, **48**, 1727–1735.
13 X. Huang, T. M. Bergsten and J. T. Groves, *J. Am. Chem. Soc.*, 2015, **137**, 5300–5303.
14 S. Biswas and A. N. Biswas, High-Valent Oxomanganese Complexes of Relevance in Oxyfunctionalization of Hydrocarbons, in *Handbook of CH-Functionalization*, ed. M. Debabrata, Wiley-VCH, 2022.
15 O. Y. Lyakin, R. V. Ottenbacher, K. P. Bryliakov and E. P. Talsi, *Top. Catal.*, 2013, **56**, 939–949.
16 (*a*) S. P. de Visser, F. Ogliaro, Z. Gross and S. Shaik, *Chem. – Eur. J.*, 2001, **7**, 4954–4960; (*b*) F. De Angelis, N. Jin, R. Car and J. T. Groves, *Inorg. Chem.*, 2006, **45**, 4268–4276; (*c*) D. Balcells, C. Raynaud, R. H. Crabtree and O. Eisenstein, *Inorg. Chem.*, 2008, **47**, 10090–10099.
17 E. Gallo, E. Solari, N. Re, C. Floriani, A. Chiesi-Villa and C. Rizzoli, *Angew. Chem., Int. Ed. Engl.*, 1996, **35**, 1981–1983.
18 V. A. Larson, B. Battistella, K. Ray, N. Lehnert and W. Nam, *Nat. Rev. Chem.*, 2020, **4**, 404–419.
19 (*a*) J. T. Groves and M. K. Stern, *J. Am. Chem. Soc.*, 1988, **110**, 8628–8638; (*b*) J. T. Groves, J. Lee and S. S. Marla, *J. Am. Chem. Soc.*, 1997, **119**, 6269–6273; (*c*) R. Zhang and M. Newcomb, *J. Am. Chem. Soc.*, 2003, **125**, 12418–12419; (*d*) O. S. Oablyasova, V. Zamudio-Bayer, M. Flach, M. da Silva Santos, J. T. Lau and K. Hirsch, *Phys. Chem. Chem. Phys.*, 2024, **26**, 5830–5835.
20 D. Feichtinger and D. A. Plattner, Direct Proof for O=MnV (salen) Complexes, *Angew. Chem., Int. Ed. Engl.*, 1997, **36**, 1718–1719.
21 (*a*) D. Feichtinger and D. A. Plattner, *J. Chem. Soc., Perkin Trans. 2*, 2000, 1023–1028; (*b*) D. Feichtinger and D. A. Plattner, *Chem. – Eur. J.*, 2001, **7**, 591–599.
22 (*a*) B. R. Cook, T. J. Reinert and K. S. Suslick, *J. Am. Chem. Soc.*, 1986, **108**, 7281–7286; (*b*) N. Jin and J. T. Groves, *J. Am. Chem. Soc.*, 1999, **121**, 2923–2924; (*c*) W. Nam, I. Kim, M. H. Lim, H. J. Choi, J. S. Lee and H. G. Jang, *Chem. – Eur. J.*, 2002, **8**, 2067–2071; (*d*) W. J. Song, M. S. Seo, S. DeBeer George, T. Ohta, R. Song, M.-J. Kang, T. Tosha, T. Kitagawa, E. I. Solomon and W. Nam, *J. Am. Chem. Soc.*, 2007, **129**, 1268–1277; (*e*) S. Fukuzumi, H. Kotani, K. A. Prokop and D. P. Goldberg, *J. Am. Chem. Soc.*, 2011, **133**, 1859–1869.
23 (*a*) F. M. MacDonnell, N. L. P. Fackler, C. Stern and T. V. O'Halloran, *J. Am. Chem. Soc.*, 1994, **116**, 7431–7432; (*b*) X. Wu, M. S. Seo, K. M. Davis, Y.-M. Lee, J. Chen, K.-B. Cho, Y. N. Pushkar and W. Nam, *J. Am. Chem. Soc.*, 2011, **133**, 20088–20091; (*c*) R. L. Halbach, D. Gygi, E. D. Bloch, B. L. Anderson and D. G. Nocera, *Chem. Sci.*, 2018, **9**, 4524–4528; (*d*) X.-X. Li, M. Guo, B. Qiu, K.-B. Cho, W. Sun and W. Nam, *Inorg. Chem.*, 2019, **58**, 14842–14852; (*e*) G. Gupta, M. Bera, S. Paul and S. Paria, *Inorg. Chem.*, 2021, **60**, 18006–18016; (*f*) G. Green, K. U. Ansari, T. Munikrishna, S. Ezov, D. Shamali, L.-N. Nanda, V. Gutkin, O. Cohen, D. Shimon and Y. Tulchinsky, *J. Am. Chem. Soc.*, 2025, **147**, 30647–30660.
24 T. Kurahashi, A. Kikuchi, T. Tosha, Y. Shiro, T. Kitagawa and H. Fujii, Transient Intermediates from Mn(salen) with Sterically Hindered Mesityl Groups: Interconversion between MnIV-Phenolate and MnIII-Phenoxyl Radicals as an Origin for Unique Reactivity, *Inorg. Chem.*, 2008, **47**, 1674–1686.
25 T. Kurahashi, A. Kikuchi, Y. Shiro, M. Hada and H. Fujii, *Inorg. Chem.*, 2010, **49**, 6664–6672.
26 T. Kurahashi, M. Hada and H. Fujii, *Inorg. Chem.*, 2014, **53**, 1070–1079.
27 H. Chen, R. Tagore, S. Das, C. Incarvito, J. W. Faller, R. H. Crabtree and G. W. Brudvig, *Inorg. Chem.*, 2005, **44**, 7661–7670.
28 I. Araki, K. Fukui and H. Fujii, *Inorg. Chem.*, 2018, **57**, 1685–1688.
29 G. Tarantino, T. G. Burrow, M. Aramini, M. L. Baker and C. Hammond, *ACS Catal.*, 2025, **15**, 4499–4506.
30 C. Wu, J. Chen, W. Nam and B. Wang, *Coord. Chem. Rev.*, 2025, **528**, e216429.
31 (*a*) J. P. T. Zaragoza, M. A. Siegler and D. P. Goldberg, *J. Am. Chem. Soc.*, 2018, **140**, 4380–4390; (*b*) J. R. Mayfield, E. N. Grotemeyer and T. A. Jackson, *Chem. Commun.*, 2020, **56**, 9238–9255; (*c*) Y. Lee, G. L. Tripodi, D. Jeong, S. Lee, J. Roithova and J. Cho, *J. Am. Chem. Soc.*, 2022, **144**, 20752–20762; (*d*) L. Zhang, M. S. Seo, Y. Choi, R. Ezhov, O. Maximova, D. D. Malik, M. Ng, Y.-M. Lee, R. Sarangi, Y. N. Pushkar, K.-B. Cho and W. Nam, *J. Am. Chem. Soc.*, 2023, **145**, 8319–8325.
32 (*a*) I. V. Khavrutskii, R. R. Rahim, D. G. Musaev and K. Morokuma, *J. Phys. Chem. B*, 2004, **108**, 3845–3854;

(*b*) W. M. C. Sameera and J. E. McGrady, *Dalton Trans.*, 2008, **2008**, 6141–6149; (*c*) M. E. Crestoni, S. Fornarini and F. Lanucara, *Chem. – Eur. J.*, 2009, **15**, 7863–7866; (*d*) D. F. Leto, A. A. Massie, D. B. Rice and T. A. Jackson, *J. Am. Chem. Soc.*, 2016, **138**, 15413–15424.

33 T. Kurahashi, *Inorg. Chem.*, 2018, **57**, 1066–1078.

34 Y. Ciringh, S. W. Gordon-Wylie, R. E. Norman, G. R. Clark, S. T. Weintraub and C. P. Horwitz, *Inorg. Chem.*, 1997, **36**, 4968–4982.

35 B. J. Kennedy and K. S. Murray, *Inorg. Chem.*, 1985, **24**, 1552–1557.

36 T. Kurahashi, *Inorg. Chem.*, 2015, **54**, 8356–8366.

37 Z. Li, Y. Liu, Q. Xia and Y. Cui, *Chem. Commun.*, 2017, **53**, 12313–12316.

38 B. Cheng, F. Cukiernik, P. H. Fries, J.-C. Marchon and W. R. Scheidt, *Inorg. Chem.*, 1995, **34**, 4627–4639.

39 (*a*) D. Sil, S. Bhowmik, F. S. T. Khan and S. P. Rath, *Inorg. Chem.*, 2016, **55**, 3239–3251; (*b*) D. Sil, F. S. T. Khan and S. P. Rath, *Chem. – Eur. J.*, 2016, **22**, 14585–14597.

40 M. J. Baldwin, T. L. Stemmler, P. J. Riggs-Gelasco, M. L. Kirk, J. E. Penner-Hahn and V. L. Pecoraro, *J. Am. Chem. Soc.*, 1994, **116**, 11349–11356.

41 B. Cheng, P. H. Fries, J.-C. Marchon and W. R. Scheidt, *Inorg. Chem.*, 1996, **35**, 1024–1032.

42 V. Krewald, B. Lassalle-Kaiser, T. T. Boron, C. J. Pollock, J. Kern, M. A. Beckwith, V. K. Tachandra, V. L. Pecoraro, J. Yano, F. Neese and S. DeBeer, *Inorg. Chem.*, 2013, **52**, 12904–12914.

43 J. F. J. Dippy and R. H. Lewis, *J. Chem. Soc.*, 1936, **1936**, 644–649.

44 F. G. Bordwell, *Acc. Chem. Res.*, 1988, **21**, 456–463.

45 (*a*) H. Torayama, T. Nishide, H. Asada, M. Fujiwara and T. Matsushita, *Polyhedron*, 1998, **17**, 105–118; (*b*) H. Torayama, H. Asada, M. Fujiwara and T. Matsushita, *Polyhedron*, 1998, **17**, 3859–3874; (*c*) N. A. Law, J. W. Kampf and V. L. A. Pecoraro, *Inorg. Chim. Acta*, 2000, **297**, 252–264.

46 B. C. Schardt, F. J. Hollander and C. L. Hill, *J. Am. Chem. Soc.*, 1982, **104**, 3964–3972.

47 M. C. Biesinger, B. P. Payne, A. P. Grosvenor, L. W. M. Lau, A. R. Gerson and R. S. C. Smart, Resolving surface chemical states in XPS analysis of first row transition metals, oxides and hydroxides: Cr, Mn, Fe, Co and Ni, *Appl. Surf. Sci.*, 2011, **257**, 2717–2730.

48 P. J. Pospisil, D. H. Carsten and E. N. Jacobsen, *Chem. – Eur. J.*, 1996, **2**, 974–980.

49 S. Bhaduri, A. J. Tasiopoulos, M. A. Bolcar, K. A. Abboud, W. E. Streib and G. Christou, *Inorg. Chem.*, 2003, **42**, 1483–1492.

50 D. A. Pantazis, V. Krewald, M. Orio and F. Neese, *Dalton Trans.*, 2010, **39**, 4959–4967.

51 C. Arunkumar, Y.-M. Lee, J. Y. Lee, S. Fukuzumi and W. Nam, *Chem. – Eur. J.*, 2009, **15**, 11482–11489.

52 (*a*) CCDC 2483878: Experimental Crystal Structure Determination, 2025, DOI: 10.5517/ccdc.csd.cc2pcp3w; (*b*) CCDC 2483879: Experimental Crystal Structure Determination, 2025, DOI: 10.5517/ccdc.csd.cc2pcp4x; (*c*) CCDC 2483880: Experimental Crystal Structure Determination, 2025, DOI: 10.5517/ccdc.csd.cc2pcp5y; (*d*) CCDC 2483881: Experimental Crystal Structure Determination, 2025, DOI: 10.5517/ccdc.csd.cc2pcp6z; (*e*) CCDC 2483882: Experimental Crystal Structure Determination, 2025, DOI: 10.5517/ccdc.csd.cc2pcp70.